Brazilian Journal of Geophysics 43 (2025), 2, 1-17
Brazilian Geophysical Society
ISSN 2764-8044
DOI: 10.22564/brjg.v43i2.2339

METHODOLOGY FOR 4D PETRO-ELASTIC MODELING INCLUDING ROCK-FLUID INTERACTION IN PRE-SALT CARBONATE RESERVOIR

Evângela P. A. da Silva[1], Alessandra Davolio[2],
Marcos Sebastião dos Santos[2], and Denis J.Schiozer[2]

[1]Petrobras, Santos, SP, Brazil
[2]Universidade Estadual de Campinas - UNICAMP, CEPETRO, Campinas, SP, Brazil

*Corresponding author email: evangela@petrobras.com.br

Silva, E. P. A. da: 0000-0003-1746-1295
Davolio, A.: 0000-0002-1724-9780
Santos, M. S. dos: 0009-0002-4812-6473
Schiozer, D. J.: 0000-0001-6702-104X

ABSTRACT. Brazilian pre-salt carbonates represent more than 70% of the produced hydrocarbons in Brazil, which makes them of great interest for 4D seismic studies. 4D seismic modeling is crucial to understand how production impacts the 4D seismic response. We propose including rock-fluid interaction on the traditional methodology for 4D petro-elastic modeling (generally considering only variations of pressure and fluid saturation) given the presence of CO_2 in the injected fluid. To model the rock-fluid interaction, we consider expressing the dry rock bulk and shear moduli as a function of the porosity for the monitor data. In the modeling, we focus in observing changes in the rock due to dissolution of $CaCO_3$ by the CO_2-rich injected fluid. We perform the analysis in the region around the injector wells and the results show that rock-fluid interaction favors the 4D anomalies, considering the reservoir conditions in this study. The higher ΔAI values obtained in petro-elastic modeling with rock-fluid interaction present an optimistic scenario compared to a traditional petro-elastic modeling in 4D feasibility studies and as another hypothesis that supports the interpretation of 4D anomalies.

Keywords: 4D feasibility study; CO_2-rich brine injection; 4D anomalies

INTRODUCTION

4D seismic is an indispensable tool for monitoring reservoir changes due to hydrocarbon production. The success of 4D seismic in a field depends on identifying these changes in the reservoir, which has already been shown to be feasible in pre-salt reservoirs according to published 4D interpretation works (Cruz et al., 2021; Izeli et al., 2024). Carbonate reservoirs are sensitive to chemical reactions with fluids, especially when the CO_2 is present in the reservoir, favoring a rock-fluid interaction with dissolution and/or mineral

precipitations due to water acidified in this process (Shekhar et al., 2006; Luquot and Gouze, 2009; Vialle et al., 2010; Vanorio, 2015). These chemical reactions can alter the carbonate rock framework, potentially leading to changes in the petrophysical and elastic properties of the rocks that were not originally predicted (Vanorio et al., 2010; Rodrigues et al., 2012; Morschbacher et al., 2015; Clark and Vanorio, 2016).

The experiment by Clark and Vanorio (2016) on the cores from pre-salt wells off the southeastern coast of Brazil verified that the presence of CO_2 facilitates the dissolution and transport of minerals throughout the rock. Their observations were consistent with a chemically enhanced weakening of the rock frame that generated compliance pores. The associated decrease in dry rock velocity can be approximated with linear relations that depend on porosity and effective stress.

Morschbacher et al. (2015) present several results from laboratory on outcrop samples of Indiana limestone composed mainly of calcite, which petrophysical characterization and geological description can be found in the works of Churcher et al. (1991) and Ji et al. (2012). Despite these outcrops are not considered analogous to the carbonates found in Brazilian pre-salt, they are relatively homogeneous and excellent specimens for destructive tests, such as permeation tests with damage formation according to Mohamed et al. (2010) and El Hajj et al. (2013), among others. The results of the tests realized by Morschbacher et al. (2015) showed that the mixture of water with CO_2 gas (carbonated water), when injected into samples of carbonate rocks, generates chemical reactions that can cause irreversible changes in the petro-elastic properties of the rocks. Depending on the volume of fluid percolated, these changes can become significant and can definitely modify the elastic response of the rock and, consequently, generate implications for 4D seismic response.

In this study, we combined the results obtained by Clark and Vanorio (2016) and Morschbacher et al. (2015) to include rock-fluid interaction in 4D seismic modeling and we compared these results with those obtained by traditional methodology, where only pressure and/or fluid changes are considered.

Motivation

The presence of carbonate rocks with CO_2 in the pre-salt and the use of the CO_2-rich WAG (Water Alternating Gas) injection enhanced oil recovery favors the monitoring of these reservoirs through 4D seismic.

In this context, modifications in the elastic properties of carbonate rocks due to rock-fluid interaction require including this effect in traditional 4D seismic modeling studies (pressure, fluid substitution), which assumes that the rock framework is not modified over time. Thus, the effects on the elastic properties of the rock are caused only by the interaction between the CO_2-rich fluid and the minerals of the rock framework, hence not due to geomechanical effects, which may eventually be present.

Objective

The objective of this work is to develop a methodology that include rock-fluid interaction in the petro-elastic modeling for technical feasibility studies and to support the interpretation of 4D seismic data.

With this objective, the chemical phenomena involved in the rock-fluid interaction are represented by changes in the elastic properties of the carbonate rocks. The results are analyzed in comparison with those obtained by the traditional methodology of 4D seismic modeling.

Rock-fluid interaction (RFI)

According to Clark and Vanorio, 2016, P-wave velocity variation ($\Delta V_p/V_p$) has a linear dependency with porosity, which may be a proxy for pore connectivity, reactive surface area, and/or rock strength. The authors concluded that, when a reactive fluid is injected into a rock formation, there will be a drop in the P-velocity (V_p) associated with partial fracturing of vulnerable components and/or etching of micritic phases. This manifestation of compliant porosity will lead to an increase in the sensitivity of velocity to pressure that favors overpressure detection. Any subsequent increase in pore pressure (Pp) will further reduce V_p (ignoring other factors) in a manner directly proportional to pressure as the new cracks are allowed to open (Clark and Vanorio, 2016).

The associated decrease in velocity of the dry rock can be approximated with linear relations that depend on both porosity and effective stress. Clark and Vanorio (2016) showed how the velocity slowed on the order of several percent at differential stress (30 MPa), almost proportionally decreasing with higher porosity for stromatolites and perhaps the other lithofacies.

According to Morschbacher et al. (2015), the injection of CO_2 into reservoirs can trigger complex chemical reactions, starting with the dissolution of CO_2 in water (Equation 1). The intensity of these reactions is determined by the reaction rate of calcite with the acid (Equation 2) and can be inferred by measuring variations in Ca2+ concentrations, alkalinity, pH and carbon isotopes (Riding and Rochelle, 2005).

$CO_2 + H_2O \Leftrightarrow H_2CO_3 \Leftrightarrow H+ + HCO_3-$ – dissolution of CO_2 in water (1)

$CaCO_3 + H+ \Leftrightarrow Ca_2+ + HCO_3-$ – reaction of calcite with acid (2)

The results obtained by Morschbacher et al. (2015) in permeation experiments indicate that the elastic moduli of dry rock decreased between 5% and 8%, on average, due to the effects of rock-fluid interaction in the presence of CO_2 and water. We consider these results to simulate the rock-fluid interaction (RFI) in our traditional 4D seismic modeling methodology, due to calcite predominance in the reservoir (Silva et al., 2020).

METHODOLOGY

The methodology proposed here aims to include the effect of rock-fluid interaction in feasibility studies and to support 4D interpretation (Fig. 1). The detailed workflow from this work shows the rock-fluid interaction is coupled with petro-elastic model for the monitor data.

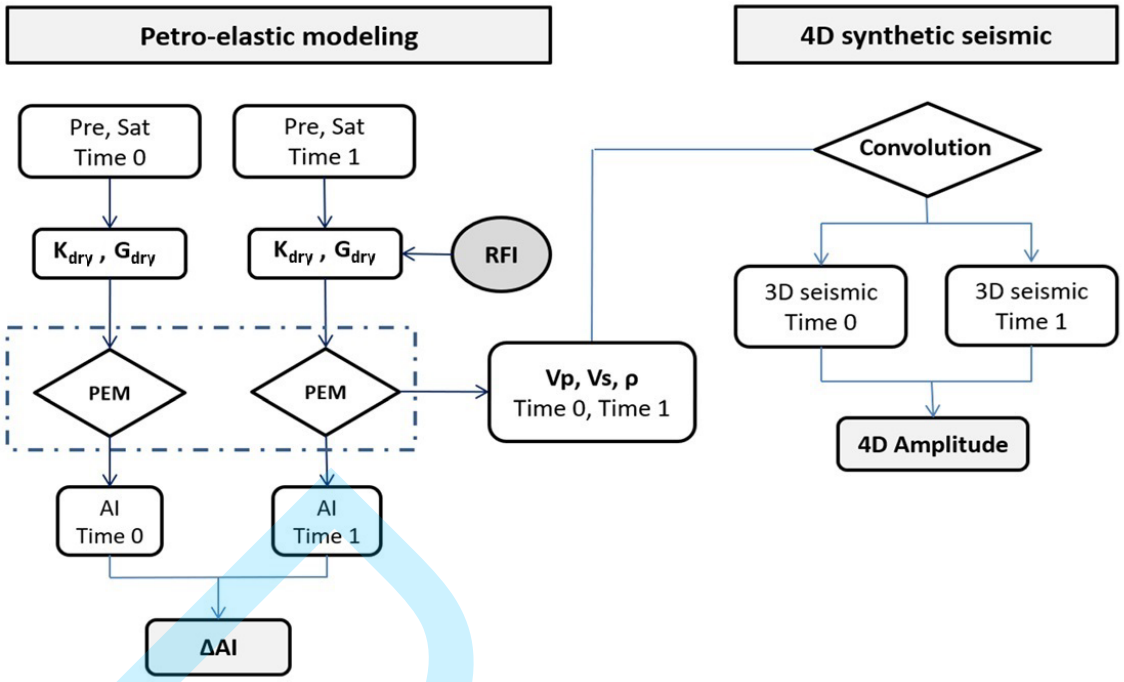

Figure 1 – Methodology used to obtain the final results in terms of ΔAI and ΔAmplitude from the application of PEM with RFI in the monitor data (Time 1).

Petro-elastic modeling (PEM)

For petro-elastic modeling, we used the properties from flow simulator (porosity, pore pressure, saturation, compressibility and density of the fluids), of a carbonate reservoir, for the Base (2017) and Monitor (2026). The reservoir is composed of microbialite (stromatolite, spherulite, laminite) and coquina and the CO_2 present in the oil corresponds to 40%.

The elastic moduli of the dry rock can be determined with well log data by rewriting the Gassmann (1951) equation isolating the bulk modulus of dry rock (K_{dry}) (Zhu and McMechan, 1990) (Equation 3). The shear modulus (G_{dry}) is considered equal to the shear modulus of the saturated rock (Gassmann, 1951) (Equation 4).

$$K_{dry} = \frac{K_{sat} * \left(\frac{\Phi * K_m}{K_{fl}} + 1 - \Phi\right) - K_m}{\frac{\Phi * K_m}{K_{fl}} + \frac{K_{sat}}{K_m} - 1 - \Phi}, \tag{3}$$

$$G_{dry} = G_{sat}, \tag{4}$$

where K_{sat} corresponds to the bulk modulus of saturated rock, Φ corresponds to porosity, K_m corresponds to the bulk modulus of the effective background, K_{fl} corresponds to the bulk modulus of the effective fluid, and G_{sat} corresponds to the shear modulus of saturated rock.

Gassmann's equation has several assumptions, as noted by Smith et al. (2003), the model assumes

that the rock is homogeneous and isotropic, which is considered a limitation when there are significant contrast in elastic stiffness (Berge, 1998). Some these limitations include: (i) the overestimation of the saturated bulk modulus, which increases with decreasing porosity, fluid compressibility, crack density (fracture density), and effective stress decrease; (ii) the pressure build-up due to CO_2 injection may lead to even great overprediction at higher pressure; and (iii) carbonates are cracked and very sensitive to stress; and (iv) one of the main issues is that the carbonates may have a higher difference in pore type and pore connectivity.

However, Adam et al. (2006) found that the brine-saturated bulk modulus for carbonates with small differential pressure dependence (round pores or vugs) is well predicted by Gassmann's equation at seismic frequencies and high differential pressures. In contrast, for carbonates that are strongly influenced by pressure (compliant pores or microcracks), Gassmann's theory does not align with observations. Therefore, understanding the geometry of the reservoir pore space can help in applying Gassmann's theory, according to the authors.

Silva et al. (2020) demonstrate that there are similar values regarding the differences in elastic attributes when comparing Gassmann's equation with the Xu and Payne (2009) models, which account for the influence of carbonate pore geometry. They show that Gassmann's equations yield equivalent results when the aspect ratios of carbonates are close to the representative values of siliciclastic rocks.

Fluid substitution*:* to model saturation changes (oil, gas, and water) in the rock, we used Gassmann (1951) equations to perform fluid substitution for seismic frequencies. Wood's (1955) suspension model is applied to obtain the acoustic properties of the fluid mixture (the compressibility moduli).

Pressure variation: for the pressure variation in the reservoir, we applied a logarithmic pressure (P_{eff}) law from the data of the normalized dry rock bulk moduli (K_{dry}) and the normalized dry shear moduli (G_{dry}) showed in Silva et al., (2020) from microbialite rocks. The lithostatic pressure was considered equal to 80 MPa to obtain effective pressure.

Rock-fluid interaction (RFI): the methodology was based on the variation of $\Delta V_p/V_p$ as a function of porosity obtained in Clark and Vanorio (2016), (Table 1), for an effective pressure of 30 MPa (reservoir pressure conditions), considering the measurements obtained in the stromatolite. We chose these measurements due to their greater variation in relation to the other samples (grainstones and spherulites) obtained by Clark and Vanorio (2016). From Table 1, we observe that the greater the porosity, the more negative the variation of $\Delta V_p/V_p$, which indicates that a more porous rock favors the reaction of brine rich in CO_2 with calcite minerals. In the study by Clark and Vanorio (2016) the variation of S-velocity ($\Delta V_s/V_s$), $\Delta K_{dry}/K_{dry}$ and $\Delta G_{dry}/G_{dry}$ with porosity was not reported, so we used the study by Morschbacher et al. (2015) where the variation of $\Delta V_p/V_p$, $\Delta V_s/V_s$, $\Delta K_{dry}/K_{dry}$ and $\Delta G_{dry}/G_{dry}$ were obtained for calcite measurements. After finding these variations in the study by Morschbacher et al. (2015), which correspond to: $\Delta V_p/V_{p\_M}$ = -5.4%, $\Delta V_s/V_{s\_M}$ = -4.9%, $\Delta K_{dry}/K_{dry\_M}$ = -12% and $\Delta G_{dry}/G_{dry\_M}$ = -11%, the relationships were applied as indicated by Equations 5 and 6, obtained by Clark and Vanorio (2016):

$$\frac{\Delta K_{dry}}{K_{dry}} = \frac{\left(\frac{\left(\frac{\Delta V_p}{V_p} * \frac{\Delta K_{dry}}{K_{dry\_M}} \right)}{\frac{\Delta V_p}{V_{p\_M}}} \right)}{100}, and \quad (5)$$

$$\frac{\Delta G_{dry}}{G_{dry}} = \frac{\left(\frac{\left(\frac{\Delta V_s}{V_s} * \frac{\Delta G_{dry}}{G_{dry\_M}} \right)}{\frac{\Delta V_s}{V_{s\_M}}} \right)}{100}. \quad (6)$$

where the subscript M indicates the variations found in the study by Morschbacher et al. (2015).

The values obtained from these relationships are shown in Table 1. Thus, for $\Delta V_p/V_p$ = -1% obtained by Clark and Vanorio (2016), we have: $\Delta V_s/V_s$ = -0.91%, $\Delta K_{dry}/K_{dry}$ = -2% and $\Delta G_{dry}/G_{dry}$ = -2%; for $\Delta V_p/V_p$ = -2.25%, we have $\Delta V_s/V_s$ = -2.04%, $\Delta K_{dry}/K_{dry}$ = -5% and $\Delta G_{dry}/G_{dry}$ = -4%; for $\Delta V_p/V_p$ = -3.50%, we have $\Delta V_s/V_s$ = -3.17%, $\Delta K_{dry}/K_{dry}$ = -8% and $\Delta G_{dry}/G_{dry}$ = -7%; and, finally, for $\Delta V_p/V_p$ = -4.75%, we have $\Delta V_s/V_s$ = -4.30%, $\Delta K_{dry}/K_{dry}$ = -11% and $\Delta G_{dry}/G_{dry}$ = -9%.

Table 1 – Values of $\Delta V_p/V_p$ and porosity obtained from Clark andVanorio (2016) for the effective pressure of 30 MPa; and values calculated from $\Delta V_p/V_p$, for $\Delta V_s/V_s$, $\Delta K_{dry}/K_{dry}$, and $\Delta G_{dry}/G_{dry}$, considering the variations obtained in measurements of calcite samples by Morschbacher et al. (2015).

From Clark and Vanorio (2016)		Analogy with Morschbacher et al. (2015)		
Porosity	**$\Delta V_p/V_p$**	**$\Delta V_s/V_s$**	**$\Delta K_{dry}/K_{dry}$**	**$\Delta G_{dry}/G_{dry}$**
0.05	-1.00	-0.91	-0.02	-0.02
0.10	-2.25	-2.04	-0.05	-0.04
0.15	-3.50	-3.17	-0.08	-0.07
0.20	-4.75	-4.30	-0.11	-0.09

In Table 1, it is observed that the variations in $\Delta V_p/V_p$ and $\Delta V_s/V_s$ decrease with the higher rock porosity, as well as the variations in the elastic moduli $\Delta K_{dry}/K_{dry}$ and $\Delta G_{dry}/G_{dry}$, which can reduce up to 11% and 9%, respectively, at porosities of 20%. In this study, no variation in porosity was considered, except for in the elastic moduli of the rock.

Figure 2 shows the behavior of variations in $\Delta K_{dry}/K_{dry}$ and $\Delta G_{dry}/G_{dry}$ as a function of porosity, presented in Table 1, which is used in petro-elastic modeling to simulate the RFI in the injection well regions where WAG injection occurs.

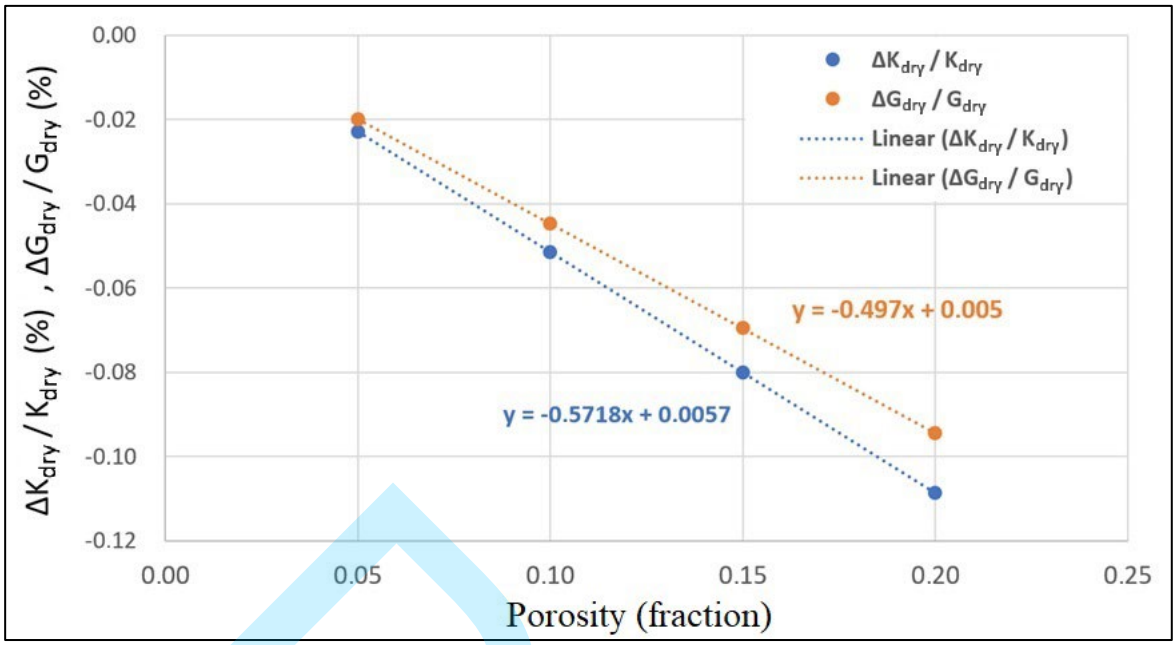

Figure 2 – Linear relationship applied to the variation of $\Delta K_{dry}/K_{dry}$ and $\Delta G_{dry}/G_{dry}$ as a function of porosity to consider the rock-fluid interaction, in the injector region, in 4D seismic modeling in the reservoir.

Scenarios in modeling

To analyze the results obtained with the inclusion of the RFI effect, four different scenarios were modeled: (i) **Pp_Sat**: traditional modeling with variation in pore pressure (Pp) and fluid saturation (ΔSw, ΔSo and ΔSg); (ii) **Pp_Sat_RFI**: traditional modeling (variation in pore pressure and fluid saturation) with the inclusion of the effect of rock-fluid interaction; (iii) **Sat_RFI**: modeling considering only the variation in fluid saturation, keeping the pore pressure constant, with the effect of rock-fluid interaction; and (iv) **Sat**: modeling only with the variation of fluid saturation, with constant pressure and without the effect of rock-fluid interaction.

The last two scenarios (Sat_RFI and Sat) are aimed to understand the seismic response in the absence of pore pressure changes with and without the inclusion of rock-fluid interaction.

The flow simulator does not include changes in porosity over time, therefore it is not a geomechanical or chemical simulator. The equations to consider the RFI are only included in the PEM, so the porosity was kept constant in all scenarios, only the elastic moduli were changed in the modeling. Figure 3 shows the porosity values in the section passing through the IG-5 and I1-WAG injection wells and the P-4 producing well, which shows the highest porosity values in the coquina. The Base (2017) and Monitor (2026) scenarios include only the water-to-gas exchange (WAG) in this study, but the reverse scenario (gas-to-water exchange (GAW)) is not considered. The RFI is applied in the petro-elastic modeling only of the monitor data (Figure 1), impacting its seismic properties and, consequently, the differences in attributes and seismic amplitude.

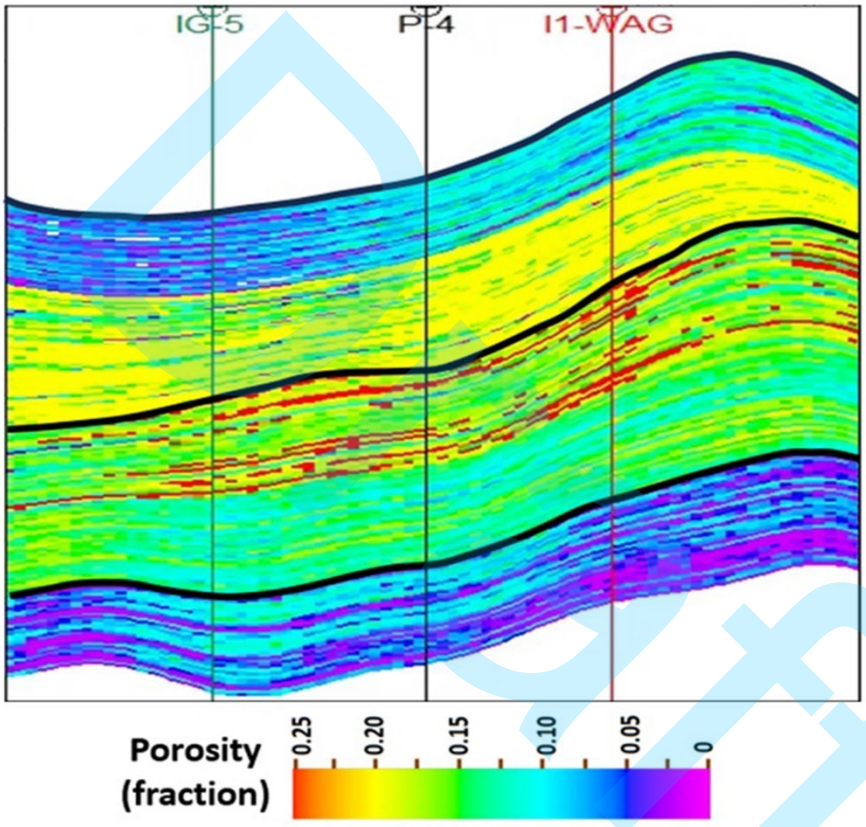

Figure 3 – Section of the reservoir showing the porosity values for the microbialite and coquina. The second horizon marks the base of the microbialite and the top of the coquina (M/C).

RESULTS AND DISCUSSION

Figure 4 shows a vertical section of the flow simulator results corresponding to: pore pressure variation (ΔPp); gas saturation variation (ΔSg); water saturation variation (ΔSw); and oil saturation variation (ΔSo). These properties are used as input in the petro-elastic modeling to obtain ΔAI, used to analyze the results.

It can be seen in Figure 4 that the depletion is below 5 MPa and this occurs practically uniformly in the reservoir; the variations in water (ΔSw) and gas (ΔSg) saturation are in the region of the injection wells (IG-5 and I1-WAG). The oil saturation variation (ΔSo) highlights the region where the oil was replaced by gas or water.

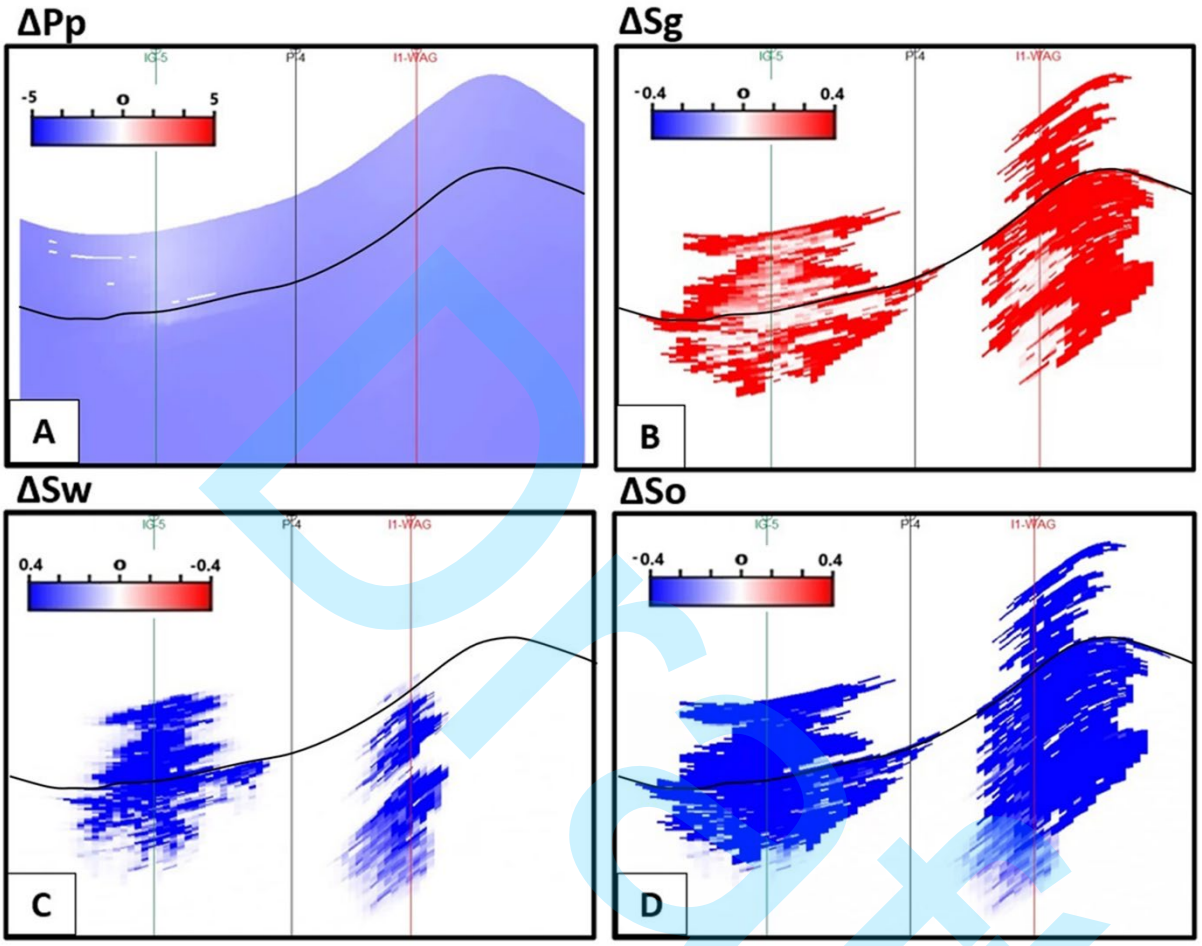

Figure 4 – Input data from the flow simulator used in petro-elastic modeling: A) pore pressure variation (ΔPp) in MPa; B) Variation in gas saturation (ΔSg) in fraction; C) Water saturation variation (ΔSw) in fraction; and D) Oil saturation variation (ΔSo) in fraction.

The variations in the bulk and shear moduli of dry rock, considering the rock-fluid interaction, are shown in Figure 5, featuring the regions with the greatest variation in moduli of ΔK_{dry} and ΔG_{dry}, occurring predominantly in coquina in well I1-WAG.

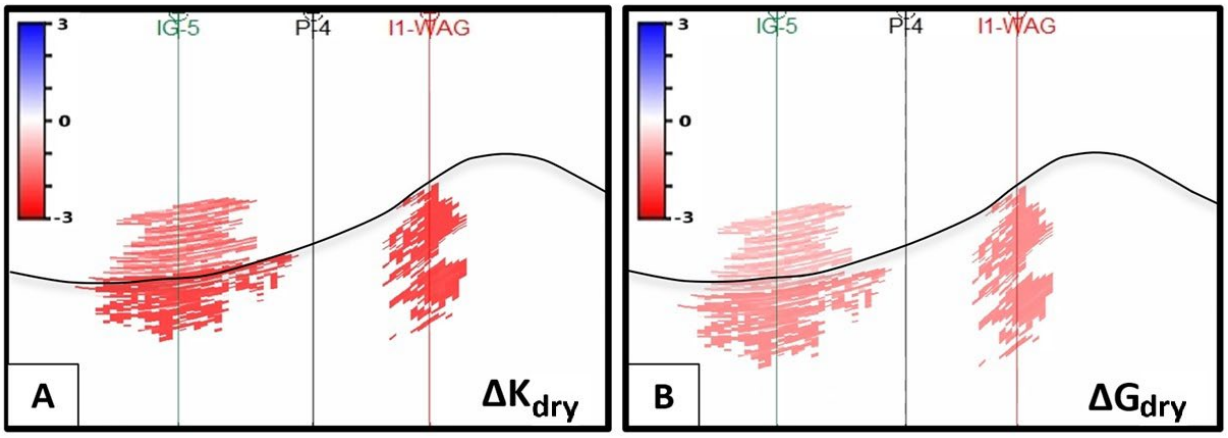

Figure 5 – Difference in the values (GPa) of K_{dry} (ΔK_{dry}) and G_{dry} (ΔG_{dry}) as a result of applying the rock-fluid interaction. Note that the variation in the ΔK_{dry} is greater than ΔG_{dry} in magnitude.

In the reservoir, the difference in absolute values of ΔK_{dry} and ΔG_{dry} between modeling without RFI and with RFI can reach 14% and 12%, respectively, as shown in Figure 6, in which it is also possible to compare the standard deviations obtained for both modules. These results are the outcome of the variation imposed in the methodology, where we saw that the variation of $\Delta K_{dry}/K_{dry}$ is greater in relation to $\Delta G_{dry}/G_{dry}$, mainly with the increase in the porosity of the rock, reaching a difference of 2% between them.

In Figure 7, the results of the scenarios with and without rock-fluid interaction are compared (Figs. 7A and 7B), in which the weakening of the elastic moduli of the dry rock is observed, thus favoring the detection of the variation in fluid saturation in the reservoir. Comparing Figures 7B and 7C (scenarios Pp_Sat_RFI and Sat_RFI), we observe that the positive ΔAI values are very similar, differing in the background values because of the pressure considered only in Figure 7B. In the Sat scenario (Fig. 7D), the absence of pressure and rock-fluid interaction favors the detection of gas saturation variation, while not intensifying water saturation variation.

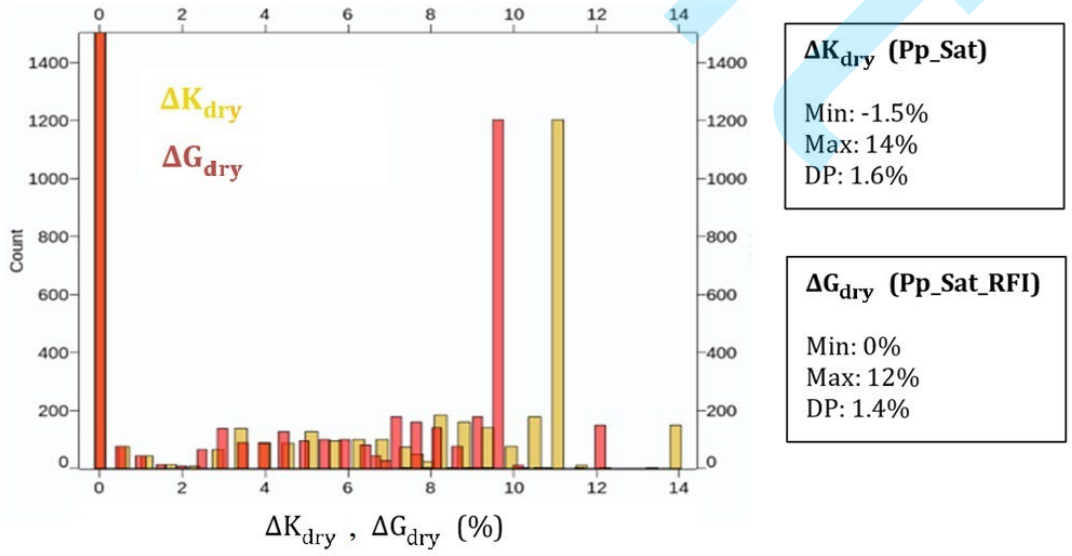

Figure 6 – Histogram with the variations of the ratio values (%) ΔK_{dry} (in yellow) and ΔG_{dry} (in red) between the scenarios without and with RFI.

From the histogram in Figure 8 and the values of ΔAI in Table 2, when comparing the scenario without and with RFI, the maximum value obtained for ΔAI increases from 1.7% to 8% in the scenarios Pp_Sat_RFI and Sat_RFI, resulting in greater 4D positive amplitude anomalies (hardening) in Figure 9B and 9C, when compared to Figure 9A.

In Figure 8 and Table 2, one may also notice that in the scenario without pressure variation and rock-fluid interaction (Sat), the minimum values obtained when compared with the other scenarios will be responsible for the 4D negative amplitude anomalies (softening) in Figure 9D, since in the absence of depletion and RFI effects, variations in gas saturation have a significant impact on the 4D seismic response in the coquina. This impact can also be observed in the region of the producing well P-4, in which we have a 4D negative anomaly (Fig. 9D), which does not occur in the other modeled scenarios (Figs. 9A, 9B, and 9C).

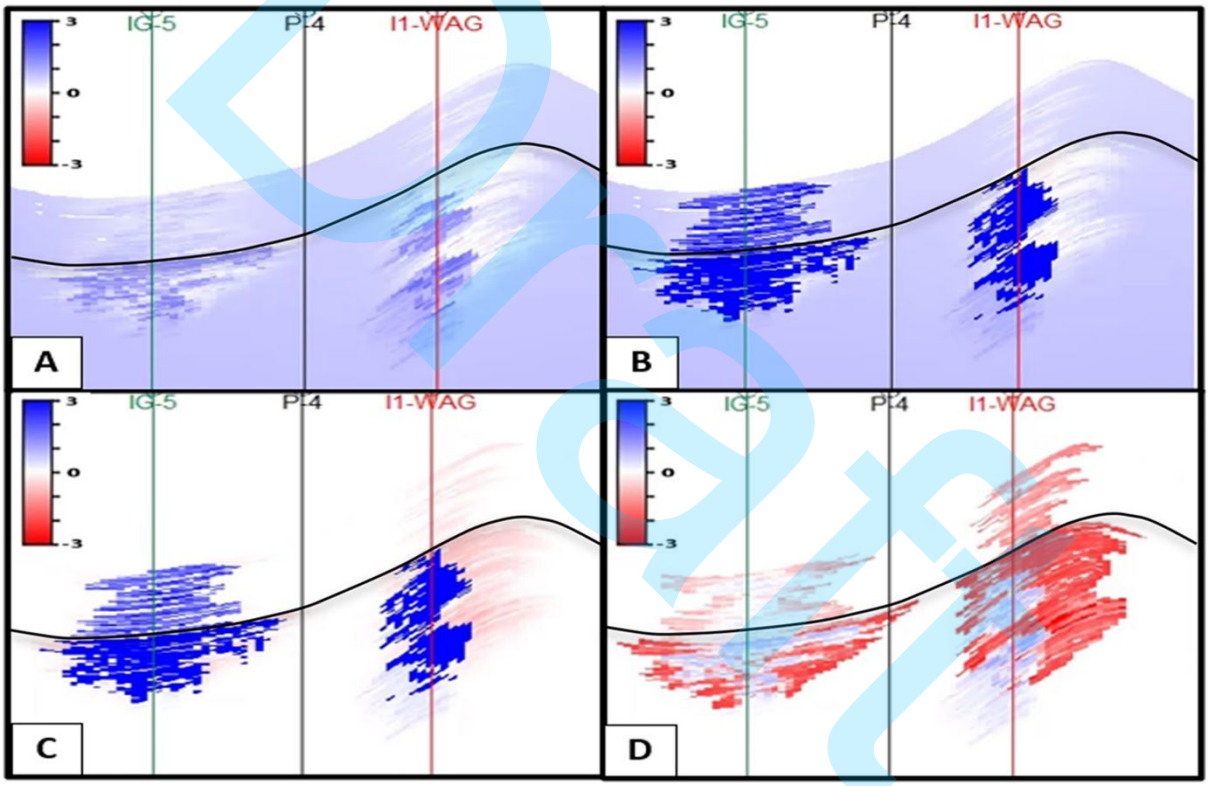

Figure 7 – ΔAI results for different scenarios of pore pressure and fluid saturation. Note in the scenarios without RFI: (A) Pp_Sat and (D) Sat, the positive 4D signal is less intense in relation to the other scenarios with RFI: (B) Pp_Sat_RFI and (C) Sat_RFI.

Figure 10 shows the relationship between porosity, input data, and the values obtained for ΔAI. This figure shows that the best porosity values above 20% are precisely those where the negative 4D anomalies appear, while for positive 4D anomalies, they already appear in porosities above 6% given the greater weakening of the elastic moduli in these regions. However, the most porous regions are precisely those with the greatest variation of ΔAI, with the variations of 4D amplitudes being positive in the scenarios with RFI (Pp_Sat_RFI and Sat_RFI) and negative for the scenario with only variation of fluid saturation

(Sat), according to the cut-off of ΔAI > 2% shown in Figure 10, since this value has shown sufficient for detectability of the 4D signal.

Table 2 – Minimum and maximum values with standard deviation for ΔAI obtained for each scenario in petro-elastic modeling. Note the maximum values in scenarios with RFI (Pp_Sat_RFI and Sat_RFI).

ΔAI - results from modeling			
Scenarios	**Minimum**	**Maximum**	**Std. Deviation**
Pp_Sat	-1.46	1.73	0.16
Pp_Sat_RFI	-1.20	8.06	0.76
Sat_RFI	-1.07	7.34	0.77
Sat	-2.89	1.07	0.48

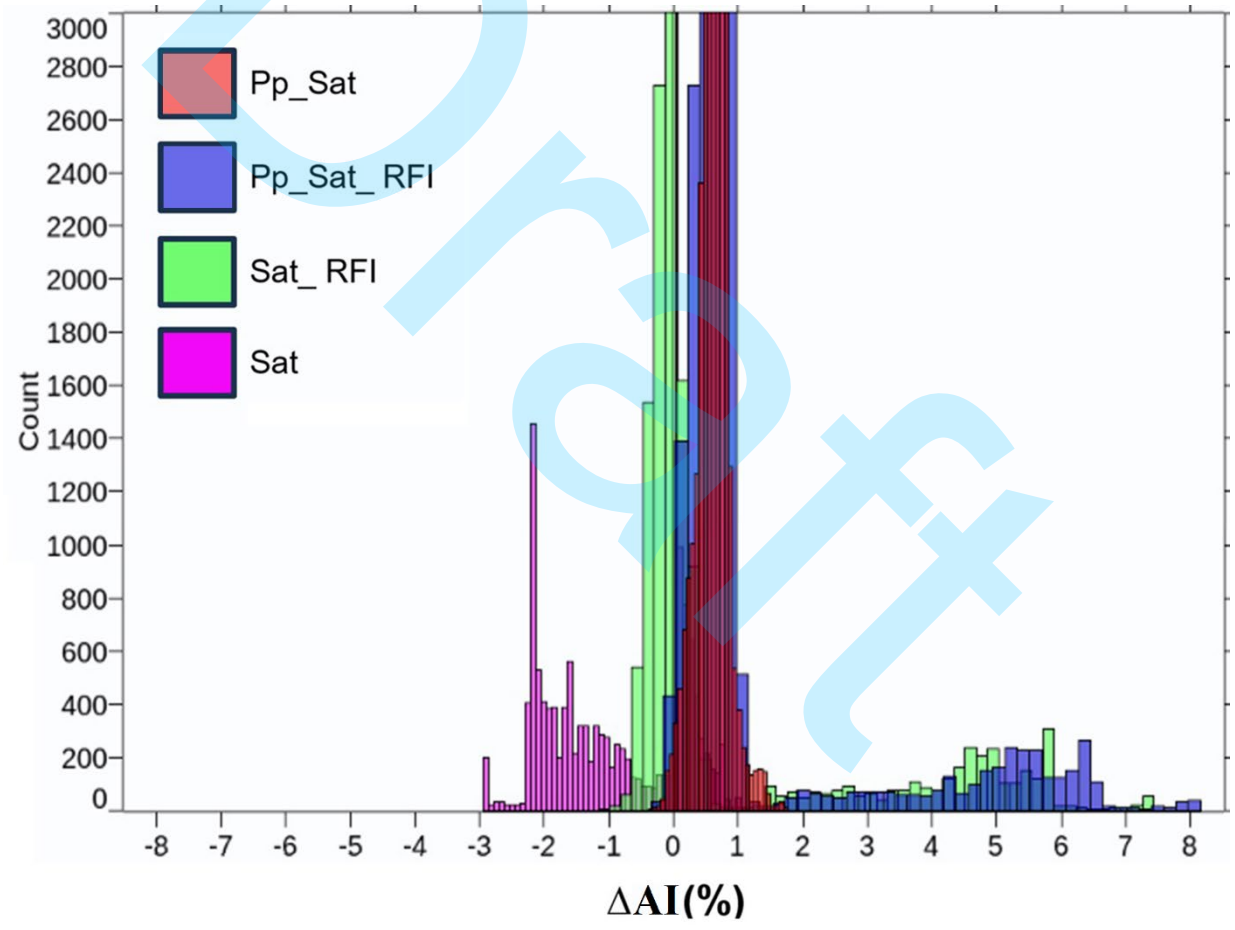

Figure 8 – Histograms with ΔAI values for the scenarios with RFI (Pp_Sat_RFI and Sat_RFI) and without RFI (Pp_Sat and Sat), where one can compare the combination between the effects of rock-fluid interaction, pore pressure, and water saturation fluids that impact the 4D response. Highlighting the histograms with maximum values of ΔAI (approximately five times higher) in scenarios with RFI compared to those without RFI.

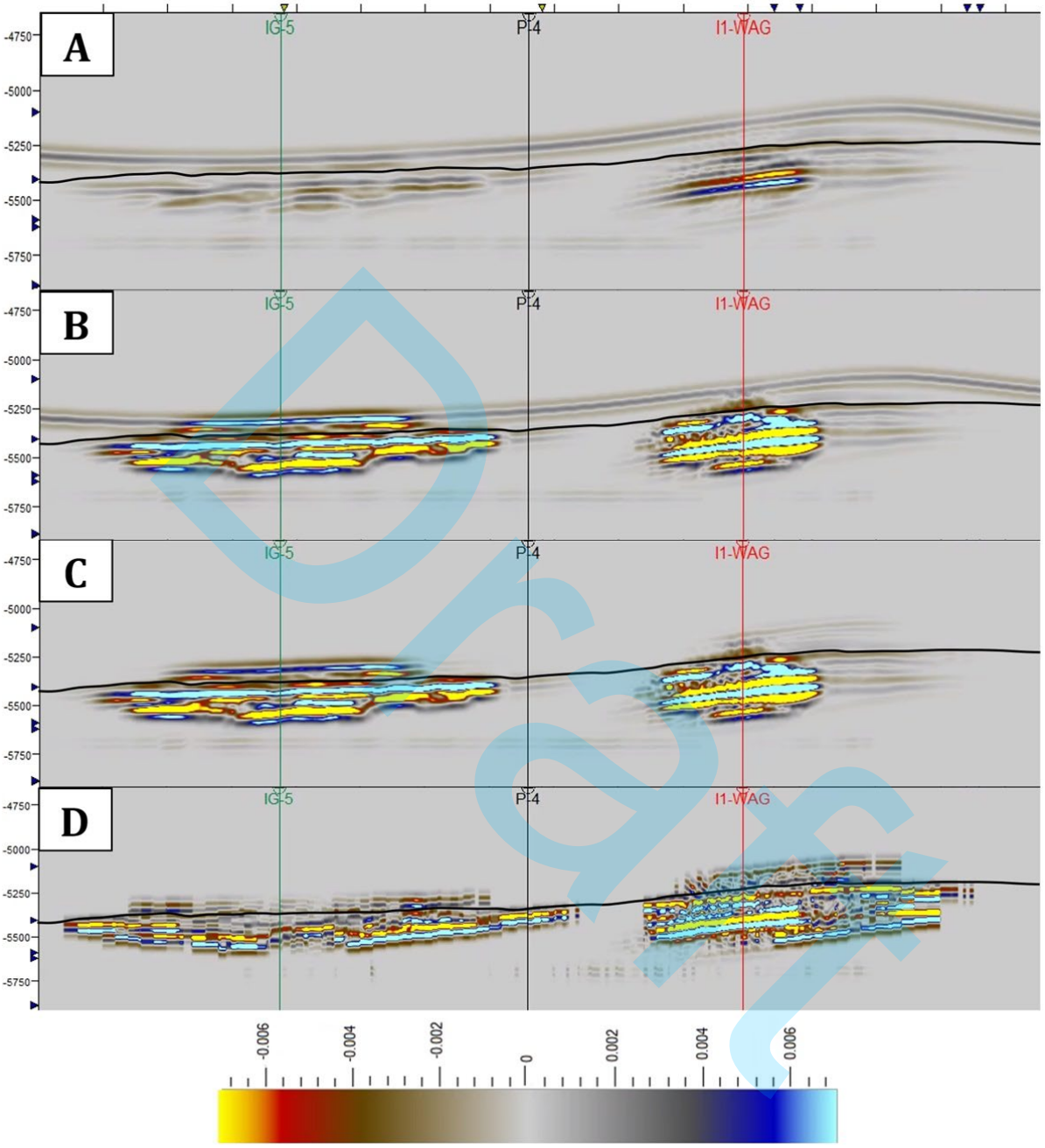

Figure 9 – 4D amplitude results for different scenarios of pore pressure and fluid saturation. Note in the scenarios without RFI: (A) Pp_Sat and (D) Sat, the 4D anomalies are lower in relation to the other scenarios with RFI: (B) Pp_Sat_RFI and (C) Sat_RFI. Highlighting the 4D anomalies in the Sat (D) scenario due to the variation in gas saturation (softening), which in the absence of pressure variation in the reservoir, generates an impact on the 4D response in the coquina.

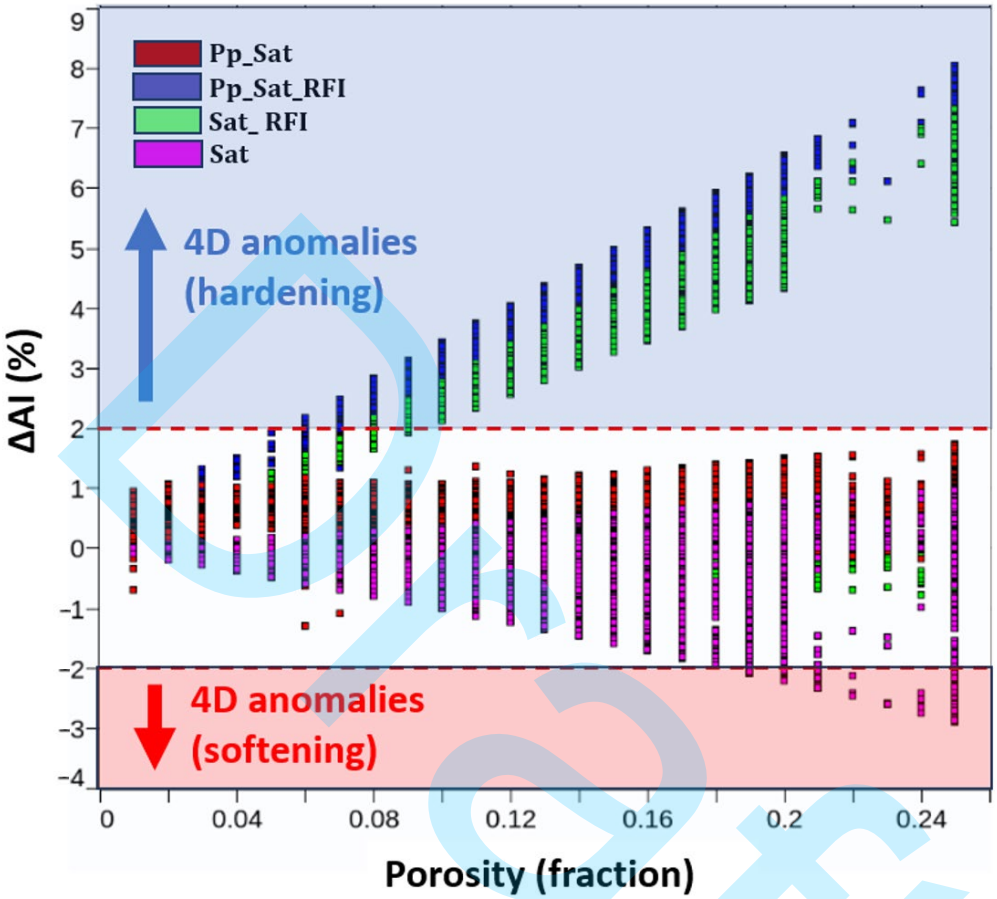

Figure 10 – Crossplot of porosity versus ΔAI shows that scenarios with RFI (Pp_Sat_RFI and Sat_RFI) present the highest values of ΔAI with positive 4D anomalies (hardening). Negative anomalies (softening) are not related to rock-fluid interaction.

CONCLUSIONS

The use of the WAG method for production of hydrocarbons in pre-salt carbonate reservoirs raises the question about the possible interaction of the rock with the fluid due to chemical processes in this system, resulting in the dissolution of minerals in the rock framework, which can result in the weakening of the elastic moduli of the rock.

The impact of these processes in the regions around injector wells and on the 4D seismic response was addressed through the application of the presented methodology, which resulted in obtaining more pronounced anomalies in the reservoir when considering the rock-fluid interaction. The results showed that the weakening of the bulk and shear moduli in the rock favored the detectability of the fluid in the pore space.

The comparison of modeling with and without variation in pore pressure shows that, in the presence of RFI, the result is practically the same in terms of 4D amplitude anomalies, as can be observed in the region of the injection wells.

In the absence of pore pressure and RFI variations in the reservoir, 4D amplitude anomalies appear both in the injector and producer regions, showing that under constant pressure conditions in the reservoir, variations in gas saturation are favored in the 4D response in the coquina reservoir. However, when in the presence of reservoir depletion, it was not possible to observe a 4D response to variations in gas saturation.

The inclusion of RFI in petro-elastic modeling in 4D feasibility studies will return optimistic results for decision-making on the most appropriate time for a seismic survey, when compared to the result in which it is not considered. In this case, we recommend presenting both scenarios to the decision maker. Its application in studies to support the 4D interpretation of real seismic data must also be evaluated, since the effect of RFI presents itself as a new hypothesis for interpreting the effects observed in the injection well regions, when other effects cannot explain the observed 4D seismic response.

ACKNOWLEDGMENTS

This work was conducted with the support of Energi Simulation and Petrobras under the ANP R&D tax as "commitment to research and development investments". The authors are grateful for the support of the Center for Energy and Petroleum Studies (CEPETRO-UNICAMP/Brazil), the Department of Energy (DE-FEM-UNICAMP/Brazil) and Research Group in Reservoir Simulation and Management (UNISIM-UNICAMP/Brazil). The authors would also like to thank the Petrobras Reservoir Geophysics Management for the unlimited support of this work; and the special colleagues support: Mônica Muzzette, Márcio Morschbacher, Ciro Climaco and Guilherme Vasquez. Finally, I thank God for the accomplishment of this work.

REFERENCES

Adam, L., M. Batzle, and I. Brevik, (2006). Gassmann's fluid substitution and shear modulus variability in carbonates at laboratory seismic and ultrasonic frequencies: Geophysics, 71, F173-F183. https//doi.org/10.1190/1.2358494.

Berge, P. A. (1998). Compressibilidade de poros em rochas, em Thimus, J.-F., Abousleiman, Y., Cheng, A.H.-D., Coussy, O., and Detournay, E., Eds., Conferência Biot sobre Poromecânica: Universite Catholique de Louvain, 351–356.

Churcher, P.L., French, P.R., Shaw, J.C., and Schramm, L.L. (1991). Rock Properties of Berea Sandstone, Baker Dolomite, and Indiana Limestone. In: SPE International Symposium on Oilfield Chemistry, Anaheim, California. SPE21044-MS. https://doi.org/10.2118/21044-MS

Clark, C. A., Vanorio, T., (2016). The rock physics and geochemistry of carbonates exposed to

reactive brines. Journal of Geophysical Research: Solid Earth, 121(3), 1497-1513. https://doi.org/10.1002/2015jb012445.

Cruz, N. M., Silva, E. P. A., Cruz, J. M., Teixeira, L. M., Costa, M. M., Oliveira, L. M., Urasaki, E. N., Bispo, T. P., Jardim, M. S., Grochau, M. H., Maul, A. (2021). Tupi Nodes Pilot: A successful 4D seismic case for Brazilian pre-salt reservoir, The Leading Edge, Special section: Latin America. 886, 896. https://doi.org/10.1190/tle40120886.1.

El Hajj, H., Odi, U., and Gupta, A. (2013). Carbonate reservoir interaction with supercritical carbon dioxide. In: International Petroleum Technology Conference, Beijing, China, IPTC 16561. https://doi.org/10.2523/IPTC-16561-Abstract.

Gassmann F. (1951). Über die Elastizität Poroser Medien. Vier. der Natur. Gesellschaf in Zürich, 96:1-23.

Izeli, M., Salgado, M., Makino, F., Silva, E. P. A., Grochau, M., Almeida, V., Dias, R., Rodrigues, C., Diniz, J., Da Silva, E. (2024). A new paradigm for the Brazilian Pre-salt reservoir monitoring through hybrid 4D seismic, EAGE 85th EAGE Annual Conference & Exhibition. Oslo, Norway. https://doi.org/10.3997/2214-4609.2024101443.

Ji, Y., Baud, P., Vajdova, V., and Wong T. (2012). Characterization of Pore Geometry of Indiana Limestone in Relation to Mechanical Compaction. Oil & Gas Science and Technology – Rev. IFP Energies nouvelles, Vol. 67 5, pp. 753-775. https://doi.org/10.2516/ogst/2012051.

Luquot, L., and Gouze, P. (2009). Experimental determination of porosity and permeability changes induced by injection of CO_2 into carbonate rocks. Chemical Geology, v. 265, 148-159. http://doi.org/10.1016/j.chemgeo.2009.03.028.

Mohamed, I.M., He, J., Mahmoud, M.A., and Nasr-El-Din, H.A. (2010). Effects of pressure, CO_2 volume, and the CO_2 to water volumetric ratio on permeability change during CO_2 sequestration. In: Abu Dhabi International Petroleum Exhibition and Conference, Abu Dhabi, UAE, SPE-136394. SPE-136394. https://doi.org/10.2118/136394-MS.

Morschbacher, M.J., Vasquez, G.F.; Justen, J.C.R., and Silveira, A.J.P.P.M. (2015). Implicações da interação rocha-fluido na geofísica de reservatórios carbonáticos. 14th International Congress of the Brazilian Geophysical Society, Rio de Janeiro, BrazilSBGf. . https://doi.org/10.1190/sbgf2015-172.

Riding, J.B., and Rochelle, C.A. (2005). The IEA Weyburn CO_2 monitoring and storage project. Final report of the European Research Team. British Geological Survey Research Report, RR/05/03, 54p.

Rodrigues, L.G., Nunes, J.P., and Guérillot, D.R. (2012). Evolution of seismic responses due to CO_2 injection in carbonates including chemical reactions and rock-physics model. ECMOR XIII – 13th European Conference on the Mathematics of Oil Recovery. Biarritz, France. EAGE. https://doi.org/10.3997/2214-4609.20143247.

Shekhar, R., Gibson Jr., R. L., Kumar, A., and Datta-Gupta, A. (2006). Seismic modeling of compositional and geochemical effects in CO_2 sequestration. SEG Expanded Abstracts, 25, 2176-2180. https://doi.org/10.1190/1.2369967.

Silva, E. P. A.; Davolio, A.; Santos, M. S.; Schiozer, D. J. (2020). 4D petroelastic modeling based

on a presalt well, Interpretation. 8, 3, T639-T649. https//doi.org/10.1190/INT-2019-0099.1.

Smith, T. M., C. H. Sondergeld, and C. S. Rai (2003). Gassmann fluid substitutions: A tutorial: Geophysics, 68, 430–440, doi:10.1190/1.1567211.

Vialle, S., Vanorio, T., and Mavko, G. (2010) Monitoring the changes of rock properties in a micritic limestone upon injection of a CO2 rich fluid. SEG Technical Program Expanded Abstracts 2010, pp. 2692-2696.

Vanorio, T. (2015). Recent advances in time-lapse, laboratory rock physics for the characterization and monitoring of fluid-rock interactions. Geophysics, v. 80, n. 2, WA49-WA59. https://doi.org/10.1190/geo2014-0202.1.

Vanorio, T., Mavko, G., Vialle S., and Spratt, K. (2010). The rock physics basis for 4D seismic monitoring of CO_2 fate: Are we there yet? The Leading Edge, v. 29, n. 2, 156-162. https://doi.org/10.1190/1.3304818.

Wood, A. W. (1955). A textbook of sound, The MacMillan Co., New York, 360 pp.

Xu, S.; Payne, M.A. (2009). Modeling elastic properties in carbonate rocks. The Leading Edge, 28, 66-74. https://doi.org/10.1190/1.3064148.Zhu, X., and McMechan, G.A., (1990). Direct estimation of the bulk modulus of the frame in a fluid-saturated elastic medium by Biot theory: 60th Ann. Internat. Mtg., Soc. Expl. Geophys., Expanded Abstracts, 787-790.

Silva, E. P. A. da: Conceptualization (lead), writing (lead), review (lead) and editing (lead); **Davolio, A.:** Conceptualization (equal), writing (supporting), review (supporting) and editing (supporting); **Santos, M. S. dos:** Conceptualization (equal), writing (supporting), review (supporting) and editing (supporting); **Schiozer, D. J.:** Conceptualization (supporting), writing (supporting), review (supporting) and editing (supporting).